Article

Low-Molecular-Weight Gelators: Elucidating the Principles of Gelation Based on Gelator Solubility and a Cooperative Self-Assembly Model

Andrew R. Hirst, Ian A. Coates, Thomas R. Boucheteau, Juan F. Miravet, Beatriu Escuder, Valeria Castelletto, Ian W. Hamley, and David K. Smith

J. Am. Chem. Soc., **2008**, 130 (28), 9113-9121 • DOI: 10.1021/ja801804c • Publication Date (Web): 18 June 2008

J|A|C|S
ARTICLES

Published on Web 06/18/2008

Low-Molecular-Weight Gelators: Elucidating the Principles of Gelation Based on Gelator Solubility and a Cooperative Self-Assembly Model

Andrew R. Hirst,[†] Ian A. Coates,[†] Thomas R. Boucheteau,[†] Juan F. Miravet,*[,‡] Beatriu Escuder,[‡] Valeria Castelletto,[§] Ian W. Hamley,[§] and David K. Smith*[,†]

Department of Chemistry, University of York, Heslington, York YO10 5DD, United Kingdom, Departament de Química Inorgànica i Orgànica, Universitat Jaume I, 12071, Castelló, Spain, and School of Chemistry, The University of Reading, Whiteknights, Reading RG6 6AD, United Kingdom

Received March 11, 2008; E-mail: dks3@york.ac.uk; miravet@qio.uji.es

Abstract: This paper highlights the key role played by solubility in influencing gelation and demonstrates that many facets of the gelation process depend on this vital parameter. In particular, we relate thermal stability (T_{gel}) and minimum gelation concentration (MGC) values of small-molecule gelation in terms of the solubility and cooperative self-assembly of gelator building blocks. By employing a van't Hoff analysis of solubility data, determined from simple NMR measurements, we are able to generate T_{calc} values that reflect the calculated temperature for complete solubilization of the networked gelator. The concentration dependence of T_{calc} allows the previously difficult to rationalize "plateau-region" thermal stability values to be elucidated in terms of gelator molecular design. This is demonstrated for a family of four gelators with lysine units attached to each end of an aliphatic diamine, with different peripheral groups (Z or Boc) in different locations on the periphery of the molecule. By tuning the peripheral protecting groups of the gelators, the solubility of the system is modified, which in turn controls the saturation point of the system and hence controls the concentration at which network formation takes place. We report that the critical concentration (C_{crit}) of gelator incorporated into the solid-phase sample-spanning network within the gel is invariant of gelator structural design. However, because some systems have higher solubilities, they are less effective gelators and require the application of higher total concentrations to achieve gelation, hence shedding light on the role of the MGC parameter in gelation. Furthermore, gelator structural design also modulates the level of cooperative self-assembly through solubility effects, as determined by applying a cooperative binding model to NMR data. Finally, the effect of gelator chemical design on the spatial organization of the networked gelator was probed by small-angle neutron and X-ray scattering (SANS/SAXS) on the native gel, and a tentative self-assembly model was proposed.

Introduction

Designing molecular materials in which the self-assembled nanostructures are predetermined by the molecular architecture remains a major challenge, especially if self-assembly is to be used to control not only the size and shape of supramolecular objects but also their surface chemistry or materials function.[1] Gel-phase materials constructed from low molecular weight building blocks that assemble into fibrillar nanostructures have been of particular recent interest.[2] The development of this field of nanoengineering is exemplified by the recent applications of molecular gels[3] in the fields of tissue engineering,[4] biomineralization,[5] and molecular electronics.[6] However, it is still questionable whether the structure−activity relationships that underpin self-assembly into gels are fully understood; such an understanding would better enable the ab initio design of systems in which molecular modification would control nanoscale assembly and ultimately endow specific materials function. Indeed, despite the explosive growth in the number of structurally diverse small molecule gelators (e.g., systems based on

[†] University of York.
[‡] Universitat Jaume I.
[§] The University of Reading.

(1) *Organic Nanostructures*; Atwood, J. L., Steed, J. W., Eds.; Wiley−VCH: Weinheim, Germany, 2008.
(2) (a) Terech, P., Weiss, R. G., Eds. *Molecular Gels: Materials with Self-Assembled Fibrillar Networks*; Springer: Dordrecht, The Netherlands, 2006. (b) Smith, D. K. Molecular Gels: Nanostructured Soft Materials. In *Organic Nanostructures*; Atwood, J. L., Steed, J. W., Eds.; Wiley−VCH: Weinheim, Germany, 2008; pp 111−154. (c) Fages, F., Ed *Top. Curr. Chem.* **2005**, *256*, 1–273. (d) Smith, D. K. *Tetrahedron* **2007**, *63*, 7283–7284.
(3) Sangeetha, N. M.; Maitra, U. *Chem. Soc. Rev.* **2005**, *34*, 821–836.
(4) (a) Ellis-Behnke, R. G.; Liang, Y.-X.; You, S.-W.; Tay, D. K. C.; Zhang, S.; So, K.-F.; Schneider, G. E. *Proc. Natl. Acad. Sci. U.S.A.* **2006**, *103*, 5054–5059. (b) Silva, G. A.; Czeisler, C.; Niece, K. L.; Beniash, E.; Harrington, D. A.; Kessler, J. A.; Stupp, S. I. *Science* **2004**, *303*, 1352–1355. (c) Yang, Z.; Liang, G.; Ma, M.; Abbah, A. S.; Lu, W. W.; Xu, B. *Chem. Commun.* **2007**, 843–845.
(5) (a) van Brommel, K. J. C.; Friggeri, A.; Shinkai, S. *Angew. Chem., Int. Ed.* **2003**, *42*, 980–999. (b) Sada, K.; Takeuchi, M.; Fujita, N.; Numata, M.; Shinkai, S. *Chem. Soc. Rev.* **2007**, *36*, 415–435.
(6) (a) Fukushima, T.; Asaka, K.; Kosaka, A.; Aida, T. *Angew. Chem., Int. Ed.* **2005**, *44*, 2410–2413. (b) Puigmartí-Luis, J.; Laukhin, V.; Pérez del Pino, Á.; Vidal-Gancedo, J.; Rovira, C.; Laukhina, E.; Amabilino, D. B. *Angew. Chem., Int. Ed.* **2007**, *46*, 238–241.

saccharides,[7] peptides and ureas,[8] nucleobases,[9] steroid derivatives,[10] dendrimers,[11] etc.), and their high-tech applications, a fundamental understanding of the particularities and characteristics of molecular self-assembly and gelation is still, somewhat surprisingly, limited. The difficulties associated with understanding the mechanism of gelation from first principles are exemplified by the fact that a significant research effort is still devoted to identifying potential gelator molecular architectures by screening large numbers of compounds as well as testing a wide range of solvents that may be suitable for supporting gel-phase networks.

The development of useful models to understand the assembly of molecules into molecular-scale fibrils and the mechanism of fibril−fibril interaction to yield a sample-spanning network is a particularly important topic.[12] One-dimensional assembly and associated network formation underpins the pathology of neurodegenerative disorders such as Alzheimer's disease, the mechanism of which is sensitive to the precise molecular structure and has been extensively investigated.[13] Notably, in important recent research, a few groups have developed practically useful models of gelation to explain the transformation of small-molecule gelators into three-dimensional sample-spanning networks, with the formation of small molecule gels primarily having been understood in terms of a mechanism involving the nucleation and growth of a gel network. Aggeli et al.[14] have linked the molecular structure of a diverse library of peptide molecules to hierarchical gel formation and developed a self-assembly model based on a theoretical statistical mechanical model. In a key recent study, Meijer and co-workers[15] developed a model to study the early and advanced self-assembly stages of oligo(*p*-phenylenevinylene) derivatives. In this case, self-assembly was observed to be a highly cooperative process involving homogeneous nucleation, initiated by a high-energy nonhelical aggregate of hydrogen-bonded dimers, with solvent molecules playing an explicit role in controlling the self-assembly process. The self-assembly of bis(urea)[16] and pyromellitamide[17] molecular-scale building blocks into linear assemblies has also been investigated, and once again, these processes were characterized as highly cooperative transitions from isotropic solutions to supramolecular linear assemblies, which in certain cases gave rise to macroscopic gelation. By using multiple techniques to investigate the nucleation and growth kinetics, Terech, Weiss, and co-workers[18] have also demonstrated that gelation occurs via instantaneous nucleation and the one-dimensional growth of fibers. The development of fiber−fiber interactions after fiber growth has taken place is also of interest, and with this goal in mind, studies by Fages and co-workers[19] suggested that, subsequent to the nucleation and one-dimensional fiber growth, different structural connections between fibers would be an alternative way to modulate the tertiary gel network, with either gelation or crystallization of the sample being the end result: clearly the nucleation and growth of gel fibers is, at least conceptually, related to the crystallization process. Extensive work by Liu and co-workers[20] has elucidated a gelation mechanism based on a supersaturation-driven crystallographic mismatch branching (CMB) process. In this case, a three-dimensional gel network formed when branching occurred at the tips or on the side faces of growing fibers, as controlled by the presence of suitable additives, temperature of network growth, or degree of gelator saturation. The mechanism of assembly of two-component gels[21] has also been investigated. John and co-workers[22] demonstrated that fiber growth of the gel formed by bis(2-ethylhexyl) sodium sulfosuccinate and 4-chlorophenol was underpinned by a nucleation-growth mechanism. Nandi and co-workers[23] employed a range of techniques in order to probe the effects of temperature and elucidate activation barriers to assembly of riboflavin−melamine hydrogels. Wackerly and Moore[24] demonstrated that the supramolecular polymerization of pyridyl-terminated oligomers with *trans*-dichlorobis(acetonitrile) could take place in either cooperative or stepwise (isodesmic) manner, depending on the geometry of the oligomer backbone linkages. In summary, for any given self-assembling gelator, it is highly desirable to be able to manipulate and understand the formation of large supramolecular polymeric structures and elucidate the interactions that mediate their macroscopic organization. Such studies can potentially generate gelation rules, which will have a degree of predictive power and thus enable more advanced ab initio design of gelators.

Previously, we have reported detailed studies of both one- and two-component gelation systems and focused on how varied

(7) (a) Kiyonaka, S.; Sugiyasu, K.; Shinkai, S.; Hamachi, I. *J. Am. Chem. Soc.* **2002**, *124*, 10954–10955. (b) Kiyonaka, S.; Shinkai, S.; Hamachi, I. *Chem.—Eur. J.* **2003**, *9*, 976–983.
(8) Fages, F.; Vögtle, F.; Žinić, M. *Top. Curr. Chem.* **2005**, *256*, 77–131.
(9) Araki, K.; Yoshikawa, I. *Top. Curr. Chem.* **2005**, *256*, 133–165.
(10) Žinić, M.; Vögtle, F.; Fages, F. *Top. Curr. Chem.* **2005**, *256*, 39–76.
(11) Smith, D. K. *Adv. Mater.* **2006**, *18*, 2773–2778.
(12) (a) Tanaka, F. Theory of Molecular Association and Thermoreversible Gelation. In *Molecular Gels: Materials with Self-Assembled Fibrillar Networks*; Weiss, R. G., Terech, P., Eds.; Springer: Dordrecht, The Netherlands, 2006; Chapt. 1. (b) Schmelzer, J. W. P. Kinetics of Nucleation, Aggregation and Ageing. In *Molecular Gels: Materials with Self-Assembled Fibrillar Networks*; Weiss, R. G., Terech, P., Eds.; Springer: Dordrecht, The Netherlands, 2006; Chapt. 8. (c) Liu, X. Y. *Top. Curr. Chem.* **2005**, *256*, 1–37.
(13) (a) Binder, W. H.; Smrzka, O. W. *Angew. Chem., Int. Ed.* **2006**, *45*, 7324–7328. (b) Hamley, I. W. *Angew. Chem., Int. Ed.* **2008**, *46*, 8128–8147.
(14) Aggeli, A.; Nyrkova, I. A.; Bell, M.; Harding, R.; Carrick, L.; McLeish, T. C. B.; Semenov, A. N.; Boden, N. *Proc. Natl. Acad. Sci. U.S.A.* **2001**, *98*, 11857–11862.
(15) (a) Jonkheijm, P.; van der Schoot, P.; Schenning, A. P. H. J.; Meijer, E. W. *Science* **2006**, *313*, 80–83. (b) Percec, V.; Peterca, M. *Science* **2006**, *313*, 55–56.
(16) (a) de Loos, M.; Van Esch, J.; Kellogg, R. M.; Feringa, B. L. *Angew. Chem., Int. Ed.* **2001**, *40*, 613–616. (b) Arnaud, A.; Bouteiller, L. *Langmuir* **2004**, *20*, 6858–6863. (c) Simic, V.; Bouteiller, L.; Jalabert, M. *J. Am. Chem. Soc.* **2003**, *125*, 13148–13154. (d) Bouteiller, L.; Colombani, O.; Lortie, F.; Terech, P. *J. Am. Chem. Soc.* **2005**, *127*, 8893–8898.
(17) Webb, J. E. A.; Crossley, M. J.; Turner, P.; Thordarson, P. *J. Am. Chem. Soc.* **2007**, *129*, 7155–7162.
(18) Huang, X.; Terech, P.; Raghavan, S. R.; Weiss, R. G. *J. Am. Chem. Soc.* **2005**, *127*, 4336–4344.
(19) (a) Lescanne, M.; Colin, A.; Mondain-Monval, O.; Fages, F.; Pozzo, J.-L. *Langmuir* **2003**, *19*, 2013–2020. (b) Lescanne, M.; Grondin, P.; d'Aléo, A.; Fages, F.; Pozzo, J.-L.; Mondain-Monval, O.; Reinheimer, P.; Colin, A. *Langmuir* **2004**, *20*, 3032–3041.
(20) (a) Liu, X. Y.; Sawant, P. D.; Tan, W. B.; Noor, I. B. M.; Pramesti, C.; Chen, B. H. *J. Am. Chem. Soc.* **2002**, *124*, 15055–15063. (b) Li, J. L.; Liu, X. Y.; Strom, C. S.; Xiong, J. Y. *Adv. Mater.* **2006**, *18*, 2574–2578. (c) Wang, R.-Y.; Liu, X.-Y.; Narayanan, J.; Xiong, J.-Y.; Li, J.-L. *J. Phys. Chem. B* **2006**, *110*, 25797–25802. (d) Xiong, J. Y.; Liu, X. Y.; Li, J. L.; Vallon, M. W. *J. Phys. Chem. B* **2007**, *111*, 5558–5563. (e) Wang, R. Y.; Liu, X.-Y.; Xiong, J.-Y.; Li, J.-L. *J. Phys. Chem. B* **2006**, *110*, 7275–7280.
(21) Hirst, A. R; Smith, D. K. *Chem.—Eur. J.* **2005**, *11*, 5496–5508.
(22) Tan, G.; John, V. T.; McPherson, G. L. *Langmuir* **2006**, *22*, 7416–7420.
(23) Saha, A.; Manna, S.; Nandi, A. K. *Langmuir* **2007**, *23*, 13126–13135.
(24) Wackerly, J. W.; Moore, J. S. *Macromolecules* **2006**, *21*, 7269–7276.

(molecular-scale) structural information (i.e., spacer chain,[25] stereochemistry,[26] ratio of two components,[27] and solvent[28]) controls the thermal stability of the material well above the percolation threshold. We therefore became interested in understanding the structural features that control the mechanism of gel formation and how this relates to thermal stability of the material when a sample-spanning gel network is formed. To address these issues, and in an attempt to develop a deeper conceptual understanding of gelation, this paper reports the design and investigation of four simple gelation systems in which the solubility of each gelator was tuned by sequentially modifying the peripheral groups of the structure. In this way, we hoped to control the phase separation process that transforms a molecular solution into an insoluble fibrillar gel network. We report that the thermodynamic driving force for gelation is solution saturation and that solubility plays a key role in controlling the formation of a gel. This paper provides a framework for *predicting* gel thermal parameters based on a simple, experimentally determined molecular property: solubility. Furthermore, in all cases, gelation was characterized as a cooperative self-assembly process, and importantly, the degree of cooperativity is directly determined by the molecular design ("programming") and solubility. Additionally, we report how the subtle interplay between the molecular design and the permitted spatial organization of gelator units within the fibrillar objects underpins the resulting three-dimensional gel-networks.

Results and Discussion

Design and Synthesis. The one-component gelators (Figure 1) were designed to exhibit subtle structural variations of α- and ε-amino groups of L-lysine: either all four groups were *tert*-butyl (Boc) carbamates (**4-Boc**),[29] all four were benzyl carbamates (**4-Z**), or two were Boc and two were Z (in both possible combinations, **2-αZ** and **2-εZ**). We reasoned that this approach would enable us to explore the precise influence of molecular structure on gelation mechanism in a coherent and systematic manner.[30]

The gelators were synthesized according to our previously disclosed approach,[29] which was employed in order to maintain the stereochemical integrity of the L-lysine amino acid building blocks. The designed gelators were generated by coupling the desired protected L-lysine to diaminononane by use of either 1,3-dicyclohexylcarbodiimide (DCC) or 1-ethyl-3-(3′-dimethylaminopropyl)carbodiimide (EDC) and 1-hydroxybenzotriazole (HOBt) in the presence of triethylamine (Et_3N) and ethyl acetate (EtOAc). The products, which precipitated from the reaction mixture along with dicyclohexylurea (DCU), could be extracted from the solid mixture and subsequently purified by silica column chromatography. All designed molecules were formed in excellent yields (75−80%) via this approach and were characterized by appropriate analytical methods to provide evidence of purity and identity (see Supporting Information).

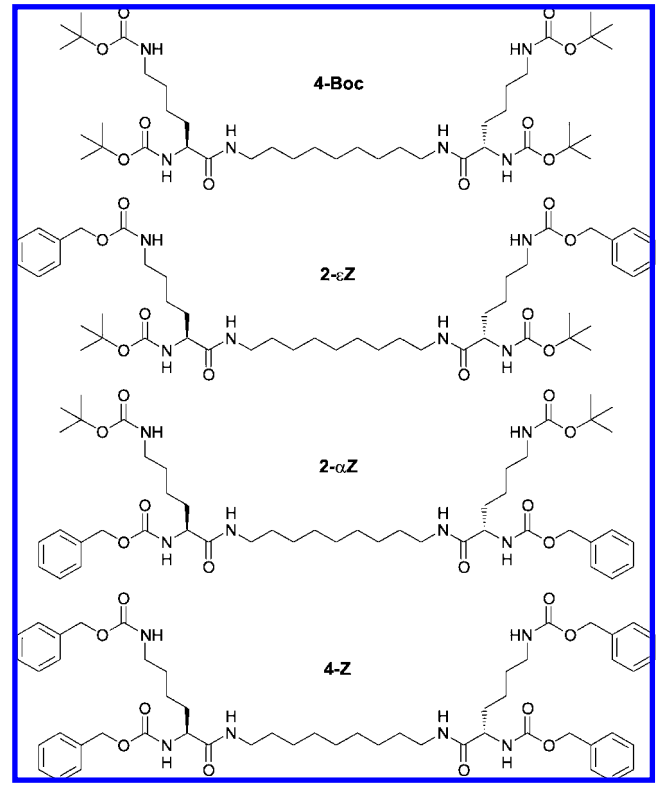

Figure 1. Structures of gelator units.

Preliminary Gelation Studies. To assess the structuring behavior of the four different gelators in a simple way, reproducible tube inversion experiments were performed.[31] This method served to define a mobile gel transition temperature (i.e., a gel "boundary") and was selected due to its simplicity and widespread use among chemists active in the field of gel-phase materials. Furthermore, there are no requirements for specialized equipment. For the purposes of this discussion, the gel boundary is considered analogous to the thermally reversible gel−sol transition temperature (T_{gel}). All the gel-phase materials reported here were thermoreversible and optically transparent, indicating good solubility under all conditions. Typically as the molar concentration was increased, T_{gel} increased until a plateau region was reached, denoted by a concentration-independent T_{gel} (Figure 2). Only in the case of the least effective gelator, **4-Boc**, was this behavior not observed. In this case, at lower concentrations (<15 mM) only partial gels or optically transparent solutions were observed, and T_{gel} values could not be determined. Strikingly, the number, nature, and position of the peripheral groups had a dramatic impact on the materials properties of the gelation systems. First, the minimum gelation concentration, MGC, measured at 25 °C was controlled by the nature of the peripheral protecting groups. Simply replacing four Boc groups with four Z groups not only reduced the MGC from 25 to 3 mM but also increased the thermal stability of the system at 40 mM from 30 to 88 °C. Furthermore, the replacement of two Boc groups by two Z groups, in combination with their

(25) Hirst, A. R.; Smith, D. K.; Feiters, M. C.; Geurts, H. P. M. *Langmuir* **2004**, *20*, 7070–7077.
(26) (a) Hirst, A. R.; Smith, D. K.; Feiters, M. C.; Geurts, H. P. M. *Chem.—Eur. J.* **2004**, *10*, 5901–5910. (b) Hirst, A. R.; Huang, B.; Castelletto, V.; Hamley, I. W.; Smith, D. K. *Chem.—Eur. J.* **2007**, *13*, 2180–2188.
(27) (a) Hirst, A. R.; Smith, D. K.; Feiters, M. C.; Geurts, H. P. M.; Wright, A. C. *J. Am. Chem. Soc.* **2003**, *123*, 9010–9011. (b) Hirst, A. R.; Smith, D. K.; Harrington, J. P. *Chem.—Eur. J.* **2005**, *11*, 6552–6559.
(28) Hirst, A. R.; Smith, D. K. *Langmuir* **2004**, *20*, 10851–10857.
(29) Gelator **4-Boc** was previously reported as a minor part of a different study: Huang, B.; Hirst, A. R.; Smith, D. K.; Castelletto, V.; Hamley, I. W. *J. Am. Chem. Soc.* **2005**, *127*, 7130–7139.
(30) Das, A. K.; Bose, P. P.; Drew, M. G. B.; Banerjee, A. *Tetrahedron* **2007**, *63*, 7432–7442.
(31) Raghavan, S. R.; Cipriano, B. H. Gel Formation: Phase Diagrams using Tabletop Rheology and Calorimetry. In *Molecular Gels: Materials with Self-Assembled Fibrillar Networks*; Weiss, R. G., Terech, P., Eds.; Springer: Dordrecht, The Netherlands, 2006; Chapt. 8.

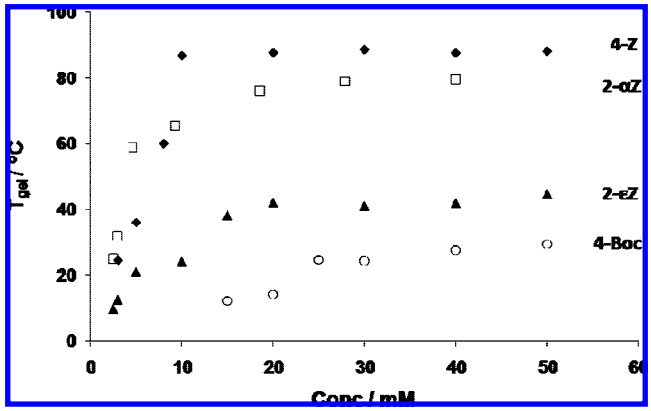

Figure 2. Thermal profiles showing the variation of gel−sol transition temperature (T_{gel}) with concentration for gelators with different peripheral groups. Solvent: toluene.

relative positions (α or ε) also played an important role in modulating the materials properties. Introducing two Z groups at the ε-position decreased the MGC value (with respect to **4-Boc**) to 10 mM, while the T_{gel} value at 40 mM was slightly increased from 30 to 45 °C. Intriguingly, introducing the two Z groups at the α-position had a considerably more pronounced effect on gelation, increasing the thermal stability, T_{gel}, to 80 °C while lowering the MGC to 3 mM. Notably, **4-Z** exhibited very similar macroscopic properties to **2-αZ**.

These observations highlight the structural importance of peripheral group chemistry on modulating the materials properties of low-molecular-weight gels.[30,32] We therefore decided to explore the gelation further, in order to gain a detailed mechanistic and theoretical understanding of the observed macroscopic gelation properties, hoping to gain an insight into the way in which subtle structural differences in gelator chemical design control both the mechanism of gelation and macroscopic thermal stability.

Importance of Gel−Sol Solubilization. As already documented in the literature, the gelation of small molecules is governed by several contributing factors, including gelator design, solvent effects, gelator concentration, and gelation temperature.[2] For a given gelation system, the last two factors can be described by the saturated state of the solution, and it can be considered that not all of the gelator will be incorporated into the solidlike fibrillar network; as such, some of the gelator will also be present in the liquidlike solution phase. This can easily be monitored by NMR methods, a technique readily available to all researchers. The observed concentration of gelator (measured via integration against an internal standard, diphenylmethane, that is also mobile within the liquidlike phase, accuracy ±5%) reflects the amount of gelator present in solution. Gelator that has been incorporated into the solidlike gel network has broadened peaks and can be considered to not contribute significantly to the observed spectrum.[33] We used this simple NMR integration approach to monitor the relative concentrations of gelator in the solidlike and liquidlike phases. The data collected for **2-εZ** are illustrated in Figure 3 as a saturation

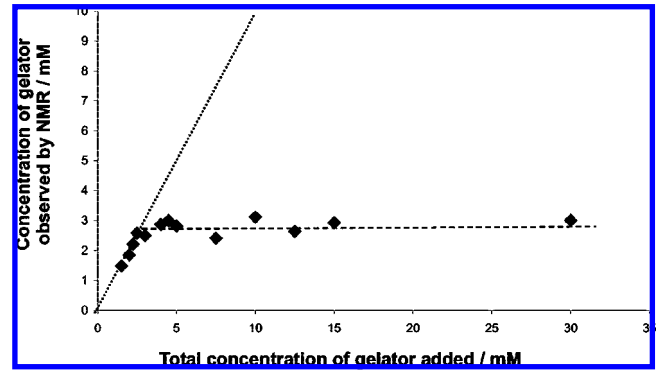

Figure 3. Plot of observed solution-phase concentration (as determined by NMR) against the total concentration of **2-εZ** system, with diphenylmethane as the internal standard. Solvent: toluene-d_8, 30 °C.

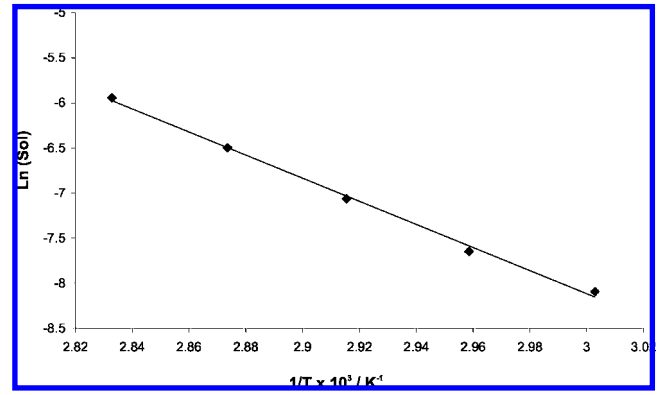

Figure 4. Plot of ln S (S = solubility, i.e., the concentration of gelator species in solution) against the reciprocal of the dissolution temperature for **4-Z** in toluene.

curve. A similar analysis was also performed for the other three gelators involved in this study.

Clearly the distinction between soluble and insoluble gelator is an important one in this type of analysis. We define species as soluble if they are visible by NMR and as insoluble aggregates if they are not visible by NMR. Of course, the nature of the transition from soluble monomers/small oligomers to insoluble aggregates is of great importance, as it will determine the extent to which this analysis is possible. We prove below (Figure 7 and associated discussion) that the aggregation behavior of these gelators is cooperative and that the alternative isodesmic model, in which there is a continuous distribution of monomer/oligomers, is not valid. This is important, because the cooperative assembly process that underpins this gelation event means that the gelator either exists as soluble monomers/small oligomers (NMR visible) or has cooperatively assembled into an insoluble supramolecular polymer with a high degree of aggregation that is NMR-silent. If, however, the assembly had been isodesmic, there would have been a poorly defined transition from monomer to extended aggregates, and this NMR treatment would have been much more complex. It should also be noted that measurements of solubility were performed at 300 and 500 MHz and provided identical results.

In the case of **2-εZ** (Figure 3), at relatively low concentrations (<3 mM), the total gelator concentration present in the system is equivalent to that of the amount of gelator being observed by NMR. Under these conditions, therefore, all of the added material can be considered to be in the liquidlike phase (i.e., in solution). However, when the total gelator concentration is

(32) (a) Hanabusa, K.; Tanaka, R.; Suzuki, M.; Kimura, M.; Shirai, H. *Adv. Mater.* **1997**, *9*, 1095–1097. (b) Coates, I. A.; Hirst, A. R.; Smith, D. K. *J. Org. Chem.* **2007**, *72*, 3937–3940. (c) Hahn, U.; Hirst, A. R.; Delgado, J. L.; Kaeser, A.; Delavaux-Nicot, B.; Nierengarten, J.-F.; Smith, D. K. *Chem. Commun.* **2007**, 4943–4945.
(33) Escuder, B.; Llusar, M.; Miravet, J. F. *J. Org. Chem.* **2006**, *71*, 7747–7752.

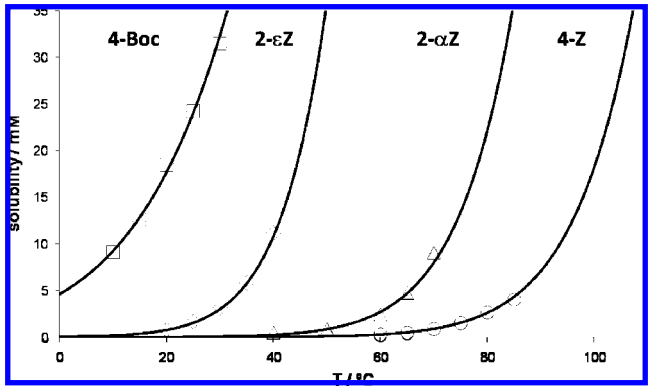

Figure 5. Effect of gelator chemical design on solubility in toluene. Symbols represent experimental data. Solid lines represent predicted solubility based on the van't Hoff equation.

Table 1. Extracted Thermodynamic and Solubility Parameters Based on the van't Hoff Plots for the Four Gelators[a]

	ΔH_{diss}, kJ mol^{-1}	ΔS_{diss}, J mol^{-1} K^{-1}	solubility at 30 °C, mM
4-Boc	44.7 (1.5)	119 (5)	31 (5)[b]
2-εZ	101.3 (1.7)	286 (6)	3 (0.5)[b]
2-αZ	102.6 (4.3)	259 (12)	0.3 (0.1)[b]
4-Z	106.4 (3.5)	252 (10)	0.007 (0.017)[c]

[a] Figures in parentheses indicate associated error. Solvent: toluene. [b] Calculated directly from ^{1}H NMR measurements at 30 °C. [c] Calculated from extrapolation of van't Hoff plot.

increased beyond 3 mM, the amount of gelator being observed by ^{1}H NMR was significantly lower than the actual amount present. This highlights the fact that the newly added material is being incorporated into the NMR-silent solidlike gel-phase network. Therefore, in this case, a concentration of ca. 3 mM corresponds to the maximum solubility of the gelator under the experimental conditions and can be considered to be the saturation point of this system. For an ideal solution, the solubility (Sol) at a given temperature can be expressed by the van't Hoff equation:

$$\ln (\mathrm{Sol}) = (-\Delta H_{diss}/RT_{eq}) + (\Delta S_{diss}/R) \quad (1)$$

ΔH_{diss} and ΔS_{diss} denote the molar enthalpy and the molar entropy for the dissolution process (i.e., gel−sol transformation), T_{eq} is the equilibrium temperature, and R is the gas constant. A typical van't Hoff plot for one of the systems under investigation (**4-Z**) is shown in Figure 4. This plot can be used to calculate ΔH_{diss} and ΔS_{diss}, and furthermore, extrapolation of this data permits the solubility (i.e., the amount of gelator in the liquidlike phase) at different temperatures to be determined. It should be noted that measurements were made at concentrations well above MGC and temperatures below T_{gel}, in order to avoid experimental conditions relating to the initial stages of gelation. The extracted thermodynamic parameters for each gelation system are listed in Table 1.

Interestingly, replacing four Boc peripheral groups with four Z groups has a profound effect on the gel−sol dissolution process. The enthalpy of dissolution, ΔH_{diss}, increases from 45 to 106 kJ mol^{-1}, confirming that the Z groups play a dominant role in maximizing favorable intermolecular forces between self-assembling units in the gel phase. The presence of four Z groups also confers a higher degree of order in the self-assembled fibrillar network as demonstrated by the fact that much more entropy is released on the dissolution of **4-Z** (ΔS_{diss} = 252 J mol^{-1} K^{-1}), than **4-Boc** (ΔS_{diss} = 119 J mol^{-1} K^{-1}). This is

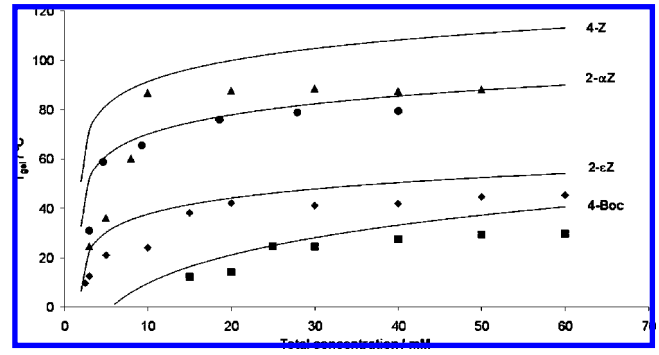

Figure 6. Effect of gelator chemical design on the gel−sol transition temperature in toluene. Symbols represent the experimental T_{gel} values based on tube inversion measurements. reflecting the breakdown of the sample-spanning network. Solid lines represent the calculated T_{calc} values based on solubility values extracted from the van't Hoff equation, relating to complete solubilization of the networked gelator.

possibly a consequence of reduced steric hindrance and more effective gelator packing. Therefore, we can conclude that introducing four Z groups to the chemical design modifies the gel−sol dissolution process by (i) enhancing the enthalpic contribution between gelator units (i.e., promoting stronger intermolecular forces) and (ii) having a higher degree of spatial organization in the insoluble gel network. The presence of four Z groups also has a profound effect on the solubility as shown in Table 1. Gelator **4-Z** has a much lower solubility at 30 °C in toluene (0.007 mM) than **4-Boc** (31 mM). This lower solubility reflects the greater enthalpic cost associated with the dissolution of gelator **4-Z**, underlining the important role of the peripheral groups on the gelator.

The precise position and number of Z groups is also an important structural design feature with respect to the gel−sol transformation. In this respect, whether the Z group is in the α-position of the lysine residue or in the ε-position subtly influences the dissolution process. Irrespective of the position of the Z groups, replacement of two Boc groups increases the enthalpy of dissolution, ΔH_{diss}, relative to **4-Boc**, from 45 to 101 kJ mol^{-1} (**2-εZ**) or 103 kJ mol^{-1} (**2-αZ**), presumably by optimizing attractive intermolecular interactions (i.e., hydrogen bonding and $\pi-\pi$ stacking) between self-assembling units. The ΔH_{diss} values for both **2-αZ** and **2-εZ** are similar (101 and 103 kJ mol^{-1}). This might be expected as the empirical formulae of the molecules, and therefore the key functional units responsible for self-assembly, are identical. However, more entropy is released on the dissolution of **2-εZ**, suggesting that the location of the Z groups can induce subtle differences in the spatial arrangement and packing of molecules within the fibrillar network. More importantly, because of this entropic difference, the precise position of the two Z groups has a pronounced effect on the observed solubility of the system. Placing the Z groups at the α-position rather than the ε-position reduces the solubility of the system at 30 °C in toluene from 3.0 to 0.30 mM. Finally, **4-Z** has a slightly higher ΔH_{diss} than the systems with two Z groups, which leads to the significantly reduced solubility of **4-Z**.

Figure 5 plots the effective solubility of the different gelators as observed by ^{1}H NMR spectroscopy at different temperatures (points) against the theoretical fit as predicted by the van't Hoff equation using the derived thermodynamic parameters, ΔH_{diss} and ΔS_{diss} (solid lines). As would be expected, increasing the temperature increased the observed solubility of the gelator in toluene. This graph clearly demonstrates the influence of gelator

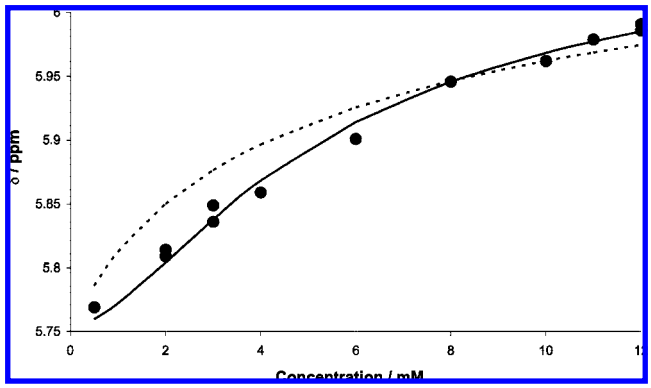

Figure 7. Concentration-dependent ^{1}H NMR shift of an N−H group of **4-Boc**, in toluene at 30 °C. The dotted line is calculated for the isodesmic model; the solid line is calculated for a cooperative model.[35,36]

Table 2. Gelator Thermal Parameters[a]

gelator	T_{gel} at 40 mM, °C	T_{calc} at 40 mM, °C	MGC at 25 °C, mM	C_{crit} at MGC, mM
4-Boc	30	35 (12)	25	4 (1)
2-εZ	45	51 (6)	10	6 (3)
2-αZ	80	86 (17)	3	3 (0.5)
4-Z	88	111 (14)	3	3 (0.5)

[a] T_{gel} was based on experimental data. T_{calc}, the calculated temperature for complete solubilization of networked gelator, was based on van't Hoff treatment of solubility data. MGC, experimental minimum gelation concentration. C_{crit}, concentration of gelator present in the fibrillar network at the MGC value (derived from NMR measurements). Numbers in parentheses indicate associated error.

design on solubility and highlights how the peripheral chemistry of the gelator controls the dissolution of the gel network.

We can further develop this approach based on solubility, in order to relate the minimum gel concentration (MGC) and the macroscopic thermal stability (T_{gel}) of the molecular gels to the thermodynamic solubility parameters of the gelators. Figure 6 attempts to relate the theoretical solubility data derived from the van't Hoff analysis (used in Figure 5) to the T_{gel} data obtained from simple gel tube inversion methodology (see Figure 2). In general terms, Figure 6 demonstrates a good correlation between the theoretical thermal profiles based on solubility (solid lines) and the experimentally measured T_{gel} data (symbols). It is noteworthy that this approach, based on gelator solubility, clearly predicts the shape of the thermal profile, including the plateau region, the existence of which has previously been difficult to rationalize.[34]

Table 2 compares key parameters from the theoretical solubility model and experimental gelation data. First, we can compare experimentally determined T_{gel} values with T_{calc} values based on the van't Hoff treatment of solubility data (T_{calc} is defined as the calculated temperature for complete solubilization of the networked gelator). It is worth noting here that T_{gel} and T_{calc} reflect subtly different things. T_{gel} corresponds to the temperature at which the gel network is partly dissolved and the remaining sample-spanning gel network becomes unable to self-support. However, T_{calc}, as mentioned above, corresponds to the temperature at which all of the gelator is disssolved. According to this, the value of T_{gel} should be lower than that of T_{calc}. The similarity of these two values, as shown in Figure 6, can be explained by bearing in mind that T_{gel} values are mainly in the steepest region of the solubility/T exponential graph. Therefore, the temperatures for partial (T_{gel}) and complete (T_{calc}) solubilization of the gel network will be similar. Subtle differences between these two values may, in the future, give insight into the mechanism of gelation for different classes of low molecular weight gelators.

Considering our own data, for **4-Boc**, the measured T_{gel} at 40 mM (in the plateau region) was 30 °C, while T_{calc} was 35 °C. For **2-εZ**, the experimental T_{gel} at 40 mM was 45 °C, while T_{calc} was 53 °C. Similarly for **2-αZ**, the measured T_{gel} at 40 mM (in the plateau region) was 80 °C, while T_{calc} was 87 °C. In each case, T_{gel} was, as expected, slightly less than T_{calc}. The behavior of **4-Z** fitted slightly less well, with T_{calc} significantly overestimating the observed T_{gel} of the system (>20 °C). The experimental difficulties associated to the low solubility of **4-Z** could cause its underestimation. For example, the solubility of this compound at 30 °C had to be determined by extrapolation of the van't Hoff plot. Overall, we argue that this van't Hoff treatment of experimental solubility data is a powerful tool to predict the line shapes of thermal profiles of low molecular weight gelators The goodness of fit demonstrates that solubility is a key parameter underpinning the gelation process that has useful predictive power. Furthermore, this treatment provides a useful parameter, T_{calc}, for comparison with experimentally observed T_{gel} values.

We then considered the experimentally determined minimum gelation concentration (MGC) values at 25 °C (Table 2). Using ^{1}H NMR as described above, we determined the effective concentration of gelator immobilized in the insoluble fibrillar network at the experimentally determined MGC value for each gelator. We defined this value as C_{crit}, the minimum amount of material required to form a fibrillar solidlike state. Remarkably, as shown in Table 2, the molar amount of gelator required in the solidlike phase (C_{crit}) was almost invariant (equivalent to a concentration of ~3−4 mM) even though the total amount of gelator required to achieve the MGC, was strongly dependent on the structural design of a given gelator (ranging from 3 to 25 mM)!

We therefore propose the definition of a useful new parameter, C_{crit}, the critical amount of gelator required for effective network formation. This is the minimum amount of material required to form a fibrillar solidlike state (assuming that all the material not visible in solution is present in the form of the solid fibrillar network). The NMR approach allows us to access the value of $C_{crit,}$ which is a true measure of the minimum amount of gelator required to form a sample-spanning three-dimensional network that can macroscopically immobilize the liquid component.

The C_{crit} value provides another mechanism by which gelator action can be directly correlated with gelator solubility. Consider, for example, the systems in which the observed MGC and C_{crit} values are identical: **2-αZ** and **4-Z**. At the MGC value, the amount of free soluble gelator is negligible due to the low solubility of these systems (Table 1): most of the gelator is therefore in the form of the solidlike network. At concentrations lower than MGC, a sample-spanning gel network is not formed by **2-αZ** and **4-Z** because the concentration of gelator is insufficient to immobilize the solvent, even though all the gelator molecules are networked. Therefore, for these cases, MGC is equivalent to C_{crit}. Conversely, for systems where MGC values deviate significantly from C_{crit} (**2-εZ** and **4-Boc**), relatively

(34) The existence of the 'plateau region' is consistently observed in our thermal characterization of gel-phase materials and has previously been queried both by referees of research papers and in research seminars. The approach employed in this paper, based on gelator solubility, clearly generates thermal stability data which matches the experimentally observed concentration dependence, and accounts for the presence of a plateau region.

Table 3. Calculated Association Constants, K_2 (Dimerization) and K_n (Oligomerization), and Downfield Shifts from ^{1}H NMR Measurements[a]

	δ free, ppm	δ max calcd, ppm	K_2	K_n	K_n/K_2
4-Boc, toluene, 30 °C	5.750	6.135 (0.016)	42 (16)	257 (19)	6
2-εZ toluene, 65 °C	5.960	6.384 (0.032)	33 (18)	246 (40)	7
2-αZ chloroform, 30 °C	6.190	6.711 (0.027)	0.8 (0.7)	35 (2)	44
4-Z chloroform, 50 °C	6.099	6.511 (0.027)	1.9 (1.0)	41 (4)	22

[a] Numbers in parentheses indicate associated error.

higher concentrations of gelator are required to form a sample-spanning network capable of immobilizing the solvent. This is because, in these systems, the greater solubilities of the gelator (Table 1) mean that the amount of free solublized gelator molecules is significant, and therefore, the point at which saturation is achieved is pushed to higher total concentrations. As such, the MGC values for these systems are higher than the C_{crit} values.

Additionally, MGC and T_{gel} can also be related through gelator solubility. We will consider the gelation systems in the plateau region of their thermal profiles, well above their characteristic MGC values. Under these conditions, T_{gel} is equivalent to the temperature at which, as a result of solubilization, the amount of solidlike networked gelator falls below the critical amount of networked gelator, C_{crit} (see Table S1 in Supporting Information). Therefore, in general terms for these gelators, the higher the MGC value is, the lower the T_{gel} value in the plateau region will be. This is because higher MGC relates to higher gelator solubility, which means that the fraction of material in the solidlike phase will drop to the critical amount of networked gelator, C_{crit}, at lower temperatures (remembering that, for the four systems reported here, C_{crit} is equivalent).

Previously, we published a full investigation of the ability of dendritic peptides to self-assemble.[29] Using variable-concentration NMR methods, we unambiguously demonstrated that this class of gelator self-assembled into gel-phase materials as a consequence of intermolecular hydrogen-bond interactions between the peptidic head groups of neighboring molecules. Here a similar trend appears: upon increasing the concentration of gelator, the observed chemical shift of the N−H group shifted downfield (Figure 7), consistent with increased intermolecular hydrogen bonding. It should be noted that clearly the N−H NMR peak does not correspond to the gelator in the solidlike gel network (as this phase is NMR-silent; see above). Instead, the NMR peak represents the formation of smaller, non-sample-spanning solution phase aggregates, a process that becomes increasingly favored at higher concentrations.

We attempted to fit the experimental concentration-dependent NMR data to two different models:[35](i) isodesmic (noncooperative) stepwise aggregation, in which each step in the assembly process has the same equilibrium constant; or (ii) cooperative aggregation, in which all association constants (K_n) are assumed to be the same except for the initial dimerization step (K_2).[16a,36] The isodesmic model failed to give an effective fit (Figure 7), but the concentration dependence of the chemical shifts could be effectively described by the cooperative model. The derived association constants are shown in Table 3. It is clear that the association constant K_n for the formation of extended self-assembled states is considerably larger than the initial dimerization constant K_2, indicating that, in all cases, the self-assembly process is highly cooperative. Indeed, in all cases, K_n/K_2 is greater than 1 (i.e., cooperative self-assembly); this is presumably because the entropic penalty of dimerization (ΔS_2) is larger than that associated with further aggregation (ΔS_n). This can be rationalized by considering the greater degree of organization that is required for dimer formation. The enthalpic terms ΔH_2 (dimer formation) and ΔH_n (self-assembly of higher order states) would be expected to be quite similar, given that they will be dominated by the noncovalent interactions formed, which should be equivalent in each case.

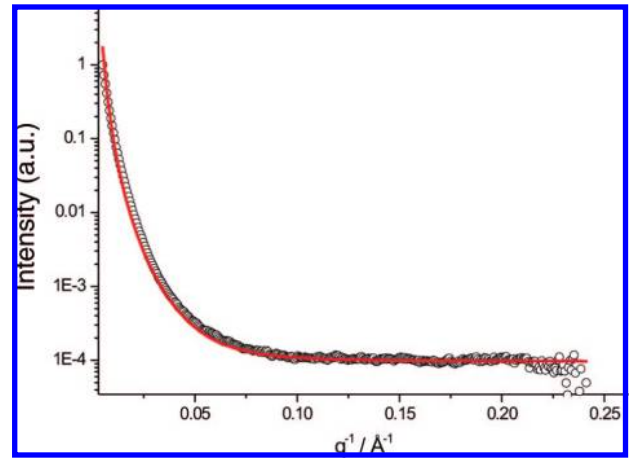

Figure 8. SAXS profile for **2-αZ** at 25 °C. (○) Experimental data; (—) modeling using eqs 2 and 3. Concentration = 8 mM, solvent = toluene.

Table 4. Parameters Used to Model the Scattering Data, Average Cylinder Radius, and Percentage of Polydispersity in R_c

gelator	R_c (Å)	σ/R_c (%)	*A*	*B*	*C*
4-Boc	18	12	1.3×10^{-3}	5.7×10^{-6}	3
2-εZ	19	27	1.9×10^{-3}	7.7×10^{-6}	3
2-αZ	70	30	9.7×10^{-5}	1.4×10^{-9}	4
4-Z	38	11	0	1.3×10^{-5}	3

The level of cooperativity appears to be dictated by the gelator structural design, although it should be noted that these experiments had to be performed in different solvents and at different temperatures in order to be able to obtain measurable NMR peaks for the N−H protons. In particular, the assembly of **4-Z** and **2-αZ** had to be monitored in chloroform due to the low solubility of these two gelators in toluene, whereas **4-Boc** and **2-εZ** could be studied in toluene. Even though chloroform represents a more competitive solvent than toluene, and therefore gives rise to lower observed association constants, the K_n/K_2 values (and hence degree of cooperativity) were significantly higher for **4-Z** and **2-αZ** than for **4-Boc** and **2-εZ**. It is therefore clear that the nature, number, and location of peripheral groups modulates the cooperativity of self-assembly, with **4-Z** and **2-αZ** exhibiting higher degrees of cooperativity.This greater cooperativity once again reflects the relatively lower solubilities of these two gelators. Therefore, the data suggest a strong correlation between solubility, level of cooperativity, and gelation properties.

(35) (a) For a review of indefinite self-association models, see Martin, R. B. *Chem. Rev.* **1996**, *96*, 3043–3064. (b) For a comparison of cooperative and noncooperative assembly processes, see Zhao, D. H.; Moore, J. S. *Org. Biomol. Chem.* **2003**, *1*, 3471–3491.

(36) Akiyama, M.; Ohtani, T. *Spectrochim. Acta, Part A* **1994**, *50*, 317–324.

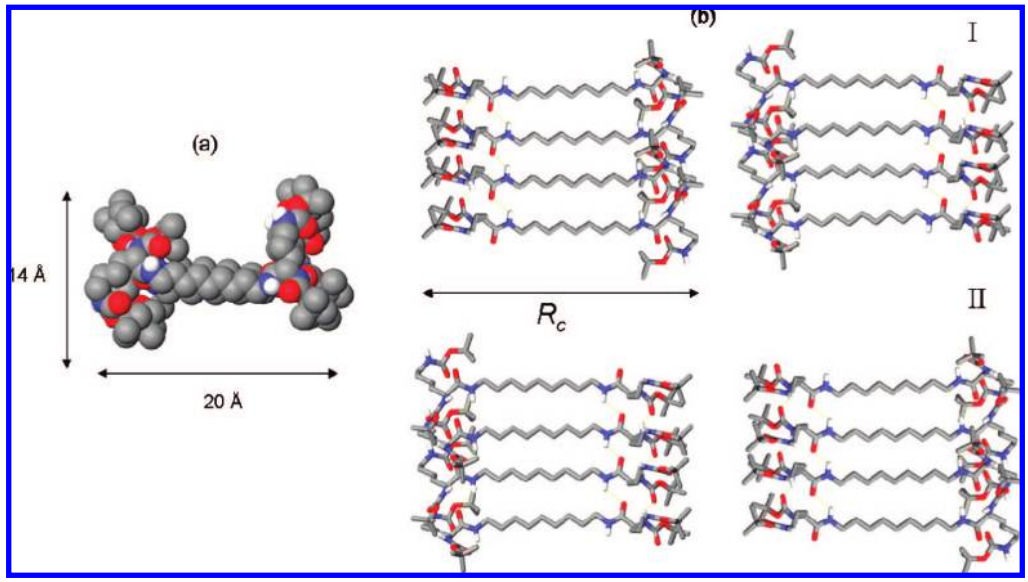

Figure 9. Dimensions and possible self-assembly behavior of **4-Boc** gelator based on experimental SANS measurements and modeled with Macromodel 9.5 program (Maestro 8.0 interface). Hydrogen atoms have been omitted for clarity. (a) CPK model representing a single **4-Boc** gelator unit. (b) Tentative self-assembly model of **4-Boc** gelator units. Dotted lines indicate intermolecular hydrogen bonding between head groups.

Structure of Network Gelator. In order to probe the precise spatial organization of the fibrillar networked gelator molecules, the gels were probed further in their native state. Small-angle neutron scattering (SANS) was used for **4-Boc** and **2-εZ**, and small-angle X-ray scattering (SAXS) was used for **2-αZ** and **4-Z**. Our experience has demonstrated that SAXS and SANS experiments provide equivalent information, making the distinction between these techniques irrelevant. In this particular work, the use of SAXS or SANS arises from circumstantial issues of equipment access and not from experimental advantages. In all cases, the characteristic dimensions of the scattering objects could be deduced by fitting the experimental data to a form factor calculated according to infinitely long flexible filaments with a circular cross-section. Network fibrillar structures were also observed for the dried xerogels by field emission gun scanning electron microscopy (FEG-SEM) (see Supporting Information). We assume that the networks observed in the micrographs represent bundles of the individual filaments characterized by SANS/SAXS and therefore represent a higher level of order. These images indicated that gelators **4-Z** and **2-αZ** appeared to form more effective interpenetrated networks. However, it should be noted that great care must be taken when ascribing structure−property relationships based on xerogel structures due to the inherent ambiguity relating to the possibility of drying effects.

Figure 8 exemplifies the results obtained for the modeling of the SAXS curve for **2-αZ** under ambient conditions at low scattering vectors. The filaments measured by SAXS/SANS were modeled according to a system of homogeneous infinite solid cylinders with polydisperse cross section:[37]

$$I(q) \propto \int_0^\infty \exp[(r - R_c)^2/2\sigma^2][J_1^2(qr)/q^3r^2]\, dr + BG \qquad (2)$$

J_1 in eq 2 is the first-order Bessel function, R_c is the average cylinder radius, and $(\sigma/R_c) \times 100$ is the percentage of polydispersity in R_c. BG in eq 2 is the background, given by

$$BG = A + Bq^{-C} \qquad (3)$$

The fitting parameters of our model are given in Table 4 for each of the different assemblies investigated.

The parameters used to model the scattering data of the four gelator systems are listed in Table 4. The results indicated that **4-Boc** and **2-εZ** gel structures consisted of self-assembled filaments with a circular cross section. Computer simulations predict a 20 Å length and a 14 Å thickness for the **4-Boc** molecule (Figure 9a). It is therefore possible to argue that the circular section of a **4-Boc** (R_c = 18 Å) filament presents two molecules lying end-by-end across the radial direction. This model is shown in Figure 9b, which shows a transversal view of the filament, across a plane containing the filament axis and perpendicular to the cross-section of the filament. It should be pointed out that models I and II are equivalent if it is assumed that the energetics of self-assembly are the same (Figure 9b). In addition, when the 14 Å molecular thickness is considered (Figure 9a), it is also possible to estimate from geometrical calculations (results not shown) that at least four **4-Boc** molecules can be radially arranged in the cross-section of the filament, giving rise to the circular geometry determined by SANS/SAXS modeling. According to the model in Figure 9b, intermolecular hydrogen bonds lie along the filament direction, explaining the anistropic nature of the self-assembled state that underpins the networked gel structure. We tentatively propose that **2-εZ** self-assembles in an analogous way to **4-Boc**, suggesting that, in this case, the introduction of two Z groups in the ε-position on the lysine residue had a minimal impact on spatial organization. Gelators **2-αZ** and **4-Z** had R_c values of 38 and 70 Å, suggesting more complex packing behaviors within the networked gelator structure and underlining the sensitivity of the self-assembly process to chemical design. Interestingly, it is these gelators, **4-Z** and **2-αZ**, that exhibit the lowest solubilities and most effective gelation. It seems likely that this may be related to the larger dimensions of the filaments observed by SAXS/SANS, with the lower solubility encouraging a greater degree of lateral interaction between molecular-scale assemblies.[38]

Conclusions

This research highlights, for the first time, how the minimum gelation concentration (MGC) and macroscopic thermal stability

(T_{gel}) of low molecular weight gelators can be rationalized in terms of the solubility and cooperative self-assembly of molecular-scale building blocks. In particular, performing a van't Hoff analysis of gelator solubility allows the generation of thermal profiles (based on T_{calc}) relating gelator concentration and thermal stability. The line shape of these calculated thermal profiles correlates with the experimentally derived T_{gel} plots, including the previously difficult to rationalize plateau region. In the case of the specific molecules investigated here, we have demonstrated that, simply by tuning the peripheral protecting groups of the gelators, we can modify the solubility of the system, which in turn controls the saturation point and the concentration at which network formation takes place. Intriguingly, we report that for these gelators, the critical concentration of gelator (C_{crit}) incorporated in the solidlike sample-spanning network at the MGC is invariant to gelator structural design. However, because some gelators have higher solubilities and therefore less preference for network formation, they appear to be less effective and require the application of higher total concentrations. Furthermore, gelator structure and solubility also modulate the level of cooperative self-assembly in a given system, as determined by applying an NMR binding model. Finally, the gelator chemical design subtly controlled the spatial organization of networked gelator as observed by SAXS/SANS. The scattering profiles obtained from the native gels were modeled and packing models for each gelator system were proposed, with greater degrees of assembly being observed for the gels that assemble with a higher degree of cooperativity.

In summary, this paper highlights the key role of solubility in influencing gelation and demonstrates that many facets of the gel-forming process depend on this vital parameter. We propose that the key, newly defined, parameters developed in this paper from considerations of gelator solubility, T_{calc} and C_{crit}, and their subtle influence on T_{gel} and MGC will be of considerable use in the field of self-assembling gel-phase materials. In particular, we believe that applying this kind of treatment to different classes of gelator will provide significant new insights into the self-assembly process.

Acknowledgment. We thank the EPSRC (EP/C520750/1) and the Ministerio de Educación y Ciencia of Spain (CTQ2006-14984) for funding this project. A.R.H. thanks Universitat Jaume I for the provision of a travel grant (Programa de promoció de la investigació 2006−2007). We also thank John Harrington [Leeds Electron Microscopy and Spectroscopy Centre (LEMAS), Department of Materials, University of Leeds] for assistance with scanning electron microscopy. We acknowledge the European Synchrotron Radiation Facility (France) for provision of synchrotron radiation facility and Dr. Narayanan Theyencheri for assistance in using beamline ID2. We thank the Leon Brillouin Laboratory (France) for provision of SANS beam time and Dr. Laurence Noirez for assistance in using station PAXY.

Supporting Information Available: Additional gelation data, scanning electron microscopic images, details of the cooperative model for NMR, details of computer modeling, and full synthesis and characterization of gelators. This material is available free of charge via the Internet at http://pubs.acs.org.

JA801804C

(37) Glatter, O.; Kratky, O. *Small Angle X-ray Scattering*; Academic Press: London, 1982.
(38) Moffat, J. R.; Smith, D. K. *Chem. Commun.* **2008**, 2248–2250.